Time-Domain Image Filtering for DIC Vibration Measurements

Time-Domain Image Filtering for DIC Vibration Measurements

P. Neri*, A. Paoli, A. V. Razionale, C. Santus

University of Pisa, Department of Civil and Industrial Engineering

*Corresponding Author email: paolo.neri@dici.unipi.it

Abstract. A time-domain filter is presented in this paper for the noise reduction of the camera images, then elaborated for the full-field 3D-DIC vibration analysis of mechanical components. The basic idea behind this filtering is to initially decompose the light signal of each pixel of the raw images, both for the left and the right cameras, with the Fast Fourier Transform (FFT). The signal is then reconstructed with the Inverse FFT by keeping the zero-order harmonic and the first harmonic and just discarding all the others, which only introduce noise contributions. The down-sampling approach is also used in combination with this filtering to reach high loading frequencies, even without (expensive) high-speed cameras, provided that a quite short exposure time is available. A cantilever aluminum plate was tested at 591 Hz, and a similar experiment was repeated on a bladed disk (or blisk) excited at high frequency, 6458 Hz, obtaining clear and smooth displacement maps even in the range of 10 microns. In the blisk application, a single blade with a significantly larger displacement amplitude was clearly observed, which could be interpreted as mistuning evidence.

1. Introduction

Digital Image Correlation (DIC) is a full-field optical technique widely adopted to retrieve motion, deformation, and shape measurements in experimental mechanics [1]. This technique has been traditionally used to investigate deformation and fracture processes, but, in recent years, its use was extended to the study of the 3D response of vibrating structures too [2]. The development of high-speed cameras made feasible the full-field analysis of high-frequencies phenomena [2-6]. However, high-speed cameras are limited by the sensor resolution, which is lower than the resolution of conventional (i.e. not high-speed) cameras. An alternative approach is represented by using conventional cameras combined with down-sampling strategies [7-9]. This approach allows the greater sensor resolution to be exploited under the limitation that the measured vibration signal is composed of a single harmonic component. However, displacements computed with sub-pixel accuracy by digital image correlation (DIC) are affected by noise, which can be introduced in the input images by the camera sensor, the non-uniform illumination, the structure of the speckle pattern (i.e., speckle size), and the adopted correlation algorithm (i.e., subset size). These issues are exacerbated by high vibration frequencies, which are usually characterized by small displacement amplitudes. A long-standing approach is based on spatial-domain and frequency-domain filters to reduce DIC measurement errors [10-13]. Image pre-filtering, before the correlation step, is adopted in [10] to minimize errors in speckle images. In [11] a Gaussian low-pass filter before the correlation process was proposed to reduce the bias error in measuring the displacements. Median adaptive low-pass

filters, Gaussian low-pass filters and notch filters were used in [12] to reduce the noise in digital image correlation-computed strain distributions. Filtering the strain distribution resulted in being the most effective noise reduction strategy. An alternative approach is provided in [14], where a post-processing tool for DIC was developed mainly for filtering the outliers in the full-field displacement data on the basis of a finite element approximation. Nevertheless, all these techniques only exploit the spatial information of the images, discarding the temporal information of the frameset, which is remarkably valuable for periodic vibrations.

In this paper, a time-domain filter is proposed, exploiting the temporal information to enhance the desired vibration measurement and reduce noise. This pre-processing allows to prepare a filtered image set, which can be subsequently processed through any of the DIC algorithms and then obtain the vibration amplitude. The proposed approach is described and validated through a relatively low-frequency measurement of a simple planar specimen. This technique is then applied to a complex 3D geometry, such as a bladed disk (blisk), which is excited at approximately 6500 Hz, measuring displacements in the range of 10 μm.

2. Materials and methods

2.1. Hardware setup

Figure 1 shows the system assembled for this experimental activity. Two Optomotive TREX cameras have been used to define a stereo optical setup. These FPGA-based cameras are equipped with a monochrome 1-inch CMOSIS imaging sensor, having a resolution of 2024×2024 pixels, a maximum full frame rate of 178 fps, and a minimum exposure time of 2 μs. Moreover, Azure Photonics 1632ZL5M C-mount varifocal (16-32 mm focal length) lenses were used to adapt the optical system to different working volumes by varying the aperture, the zoom, and the focal length. The two cameras, mounted on spherical joints connected to a bar through slides, were integrated with an off-the-shelf multimedia digital led projector (AAXA P7, 1920×1080 native resolution). Additionally, four led modules (Stratus LED 100 W module, version 3) were added to the stereo setup rig, exploiting parabolic reflectors.

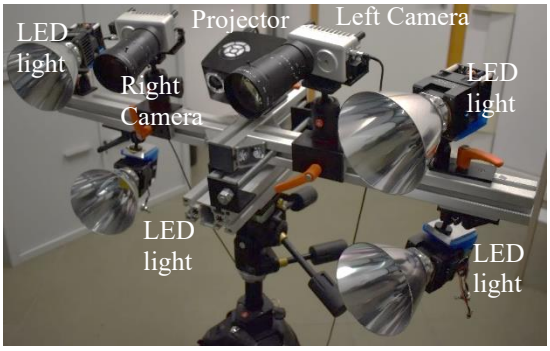

Figure 1: Developed 3D DIC system.

2.2. Measurement methodology

The described experimental setup has been used to measure the 3D displacements of high-frequency low-amplitude vibrating objects. Three different problems must be faced and solved for this purpose: 1) the acquisition of 3D points on the target surface over time, 2) the reconstruction of a high-frequency signal by using low frame rate cameras, and 3) the noise reduction affecting low-amplitude signals.

The first problem was solved using a 2D-DIC and stereo triangulation, the second by carrying out a down-sampling of the excitation signal. At the same time, a novel time-domain filter was specifically developed to reduce the noise in the measurements, as described in the following of this paper.

2.2.1. 3D acquisition. The vibrating object is sprayed with a black speckle pattern and imaged by the two cameras. Specifically, the DIC is used to separately track, over time, the corresponding points on each image stack (one for the left camera and one for the right camera), thus obtaining 2D information during the vibration phenomenon for each camera. The 3D data is then computed by the stereo-triangulation of the corresponding points between the images captured by the left and the right cameras, which need to be previously calibrated by determining intrinsic and extrinsic parameters. In this context, the most challenging task is identifying corresponding points between the left and the right images (stereo matching). Using the DIC to match image pairs deriving from an optical stereo setup (with a typical angle of 30°) was not appropriate, especially in correspondence of high curvature regions [15]. For this reason, the stereo matching task was solved by projecting a sequence of patterns (vertical and horizontal black and white stripes) exciting the object. The projection of structured light, which allows to code the scene, as in Ref. [16], was carried out only once at the beginning of the measurement process. The DIC algorithm proposed in [17] is instead separately applied on the temporal sequence of the left and the right images to track 2D points acquired from each point of view.

2.2.2. Signal down-sampling. According to the Nyquist-Shannon theorem, the highest signal frequency that can be reconstructed from a sampled signal is one-half of the sampling rate. Therefore, the adopted cameras would, theoretically, acquire up to a frequency of 89 Hz, a value that can represent a significant limit in this experimental activity. However, high-frequency signals can still be reconstructed under the hypothesis that the excitation signal contains only a single harmonic component with a known frequency [8]. The major constraint is consequently shifted from frame rate to shutter speed (or, in turn, the exposure time) which must be fast enough to prevent blurry images of moving targets. In this context, the minimum exposure time of the used TREX cameras, which is 2 μs, requires high-intensity illumination obtained with the four led modules. It is worth noting that the minimum available exposure time represents 1/50 of the period of a 10 kHz signal, thus guaranteeing the acquisition of still images even for objects vibrating at such frequency level.
In this work, the down-sampling approach described in [18] has been used to overcome the camera's frame rate limitation under the hypothesis that the displacement signal is composed of a single harmonic. The camera sampling frequency value, f_s can be selected to capture a predefined n_p number of displacement signal periods. This sampling frequency can be defined by the following equation:

$$f_s = \frac{f_v\left(n_s / n_p\right)}{1+\left(n_s / n_p\right)k} \tag{1}$$

where f_v is the actual signal frequency, n_s is the number of frames to be acquired, and k is any integer number. The k value can be set arbitrarily high, considering that the higher is k, the lower is f_s. According to Eq. 1, the down-sampled acquired signal is composed of n_p complete vibration periods, thus allowing the proper evaluation of its amplitude.

3. Time-domain filtering

The aim of the proposed filter is to exploit the time-domain information and enhance the signal acquired by the cameras before performing the DIC algorithm. Since Eq. 1 is used, the acquired images frameset will show a fictitious number of periods equal to n_p. Indeed, it is possible to extract the intensity level of a sample pixel over time and plot its value against the frame number, as shown in Fig. 2(a) for acquisition with $n_p = 1$. This plot highlights that the measured signal has a relevant mean

value, mainly depending on the scene illumination and the object color. The main contribution describes one fictitious period (actually n_p periods) overlapped to a certain noise.

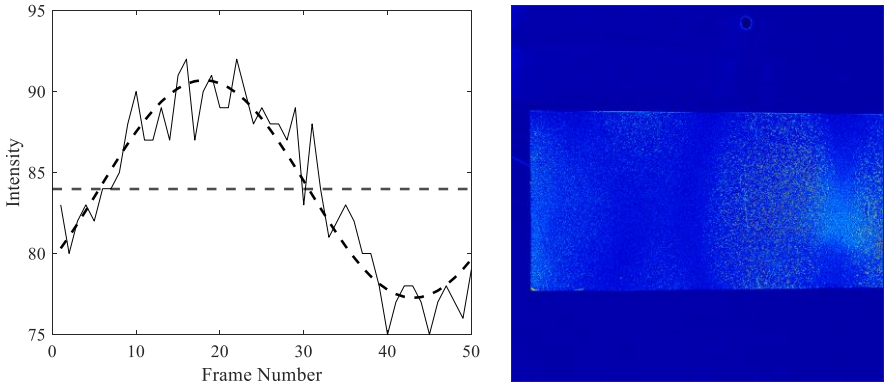

(a) (b)

Figure 2. Analysis of the frameset: (a) light intensity over time of a sample pixel and (b) amplitudes of the first harmonic.

If a pixel-wise FFT is performed on the full image, considering the whole frameset, it is reasonable to predict that the first harmonic will have a much higher amplitude with respect to the others. Indeed, Fig. 2(b) shows the pixel-wise amplitudes of the first harmonic. The figure highlights that some plate regions have higher amplitude values, while some lines have almost zero amplitude, thus denoting nodal lines of the excited deformed shape. A deeper insight into the FFT results can be obtained by looking at a zoomed view of a small picture region. Fig. 3(a) shows the selected square in the raw image, while Fig. 3(b) shows the amplitudes of the first harmonic of the corresponding pixel-wise FFT. As can be noted by comparing the two figures, the maximum amplitudes are obtained in correspondence with the speckles' edge. This is reasonable because the pixels on the edges will measure the highest variation during vibration since the grey level will change between white and black values due to the speckles' displacement. On the other hand, the pixels corresponding to the centers of the speckles will always measure a low-intensity level during small-amplitude vibrations.

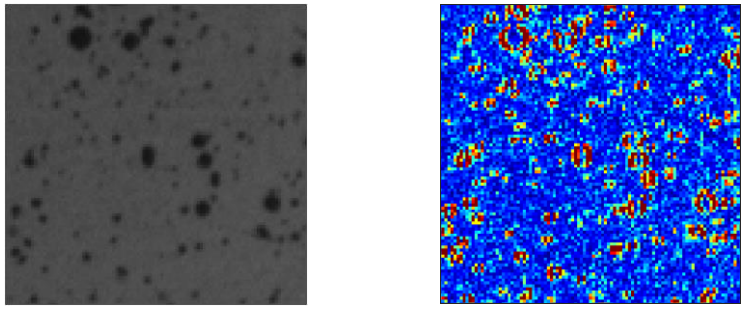

(a) (b)

Figure 3. Zoomed view of a square region: (a) raw image and (b) amplitudes of the first harmonic.

This consideration holds only in the case of the first harmonic, which is related to the physical vibration of the target. On the other hand, all the other harmonics may show relevant amplitudes, but being only related to the image noise, no specific patterns are expected. This can be verified by looking at Fig. 4, which shows the amplitude of all the harmonics 1-25 (50 frames were acquired in this example) in the same square region. In Fig. 4(a) all the amplitudes are normalized with respect to the maximum value of the first harmonic. The plot highlights that the amplitude of the first harmonic is much higher than the others. In Fig. 4(b) the amplitude of each signal contribution is normalized

with respect to the maximum of that specific harmonic. In this color scale, while the first harmonic shows the described pattern in correspondence of the speckles' edges, all the others only show a random distribution of the maxima, thus confirming that they only represent image noise.

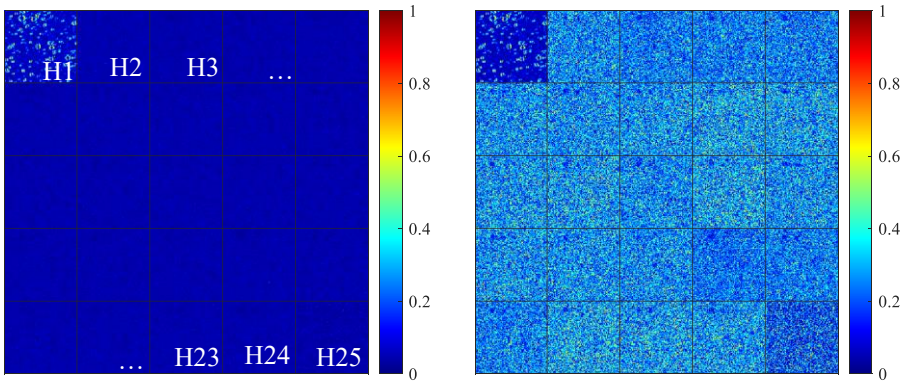

(a) (b)

Figure 4. Amplitudes of the 25 harmonics normalized with respect to: (a) the maximum of the first harmonic and (b) the maxima of each harmonic.

The noise level in the image set can be reduced by selecting the relevant harmonic component (i.e. harmonic n_p, H1, in this example) and by setting to zero all the other harmonics. The inverse FFT can be subsequently computed, thus obtaining a filtered image set only containing the information related to the desired harmonic and the noise rejected. Nevertheless, if only the n_p-th harmonic is kept, the filtered image set will lose the speckle information, as shown in Fig. 5(a), which represents the full image of the plate. This would lead the DIC algorithm to failure because the displacement detection is based on the grey levels of the speckles over time. To overcome this issue, it suffices to also keep the H0 contribution (i.e., the mean value over time) before computing the inverse FFT (IFFT). In this way, the reconstructed filtered image set will appear equal to the raw data (at the naked eye), Fig. 5(b), thus being functional for the DIC analysis. In general, the harmonics to keep for the IFFT are the zero and the n_p-th. However, as in this paper, the usual approach is to set $n_p = 1$, so the harmonics to keep are H0 and H1.

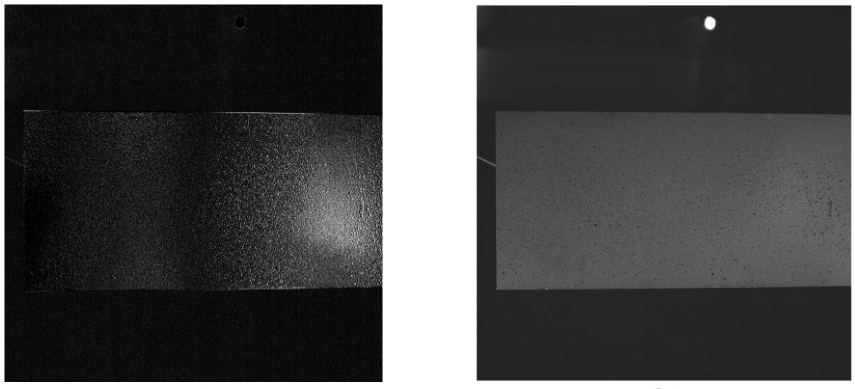

(a) (b)

Figure 5. Filtered image set by selecting: (a) only the first harmonic and (b) the first harmonic and the mean value.

4. Filter application

The described filtering approach was firstly validated on relatively low-frequency measurements by gradually reducing the load amplitude to assess the method's capabilities. Additionally, it was then applied to the high-frequency vibration measurement of a blisk.

4.1. Low-frequency validation

The method validation was performed by exploiting a cantilever aluminum plate (500 × 100 × 2 mm), vibrating at 591 Hz. One end of the plate was mounted to a shaker, while the other end was acquired by the DIC system (measurement area 220×220 mm). Firstly, a high load level was applied to the plate (corresponding to a supply voltage of 1 V to the shaker). A large-amplitude response was observed, which was properly measurable by the system even without any filtering. This allowed obtaining a reference displacement map to be used for comparison in the subsequent elaborations. The map corresponding to the maximum of the displacements' magnitude, obtained elaborating the unfiltered images, is shown in Fig. 6(a). The displacements overtime of a few points at the plate's free end (with maximum displacements) were additionally extracted and plotted in Fig. 6(c). As can be seen, the displacement is well characterized by the first harmonic component (one full period). Nevertheless, a relevant noise level can be noted, which is obviously more significant near the minima of the displacement (nodal lines). On the other hand, Fig. 6(b) shows the results obtained by processing the filtered image set. As can be seen, the map is smoother with respect to Fig. 6(a), especially close to the nodal lines. This is further confirmed by looking at Fig. 6(d), which shows the displacement over time of the plate's free end along the three directions. Here, the noise level is drastically reduced, and the dominant first harmonic is clearly evident.

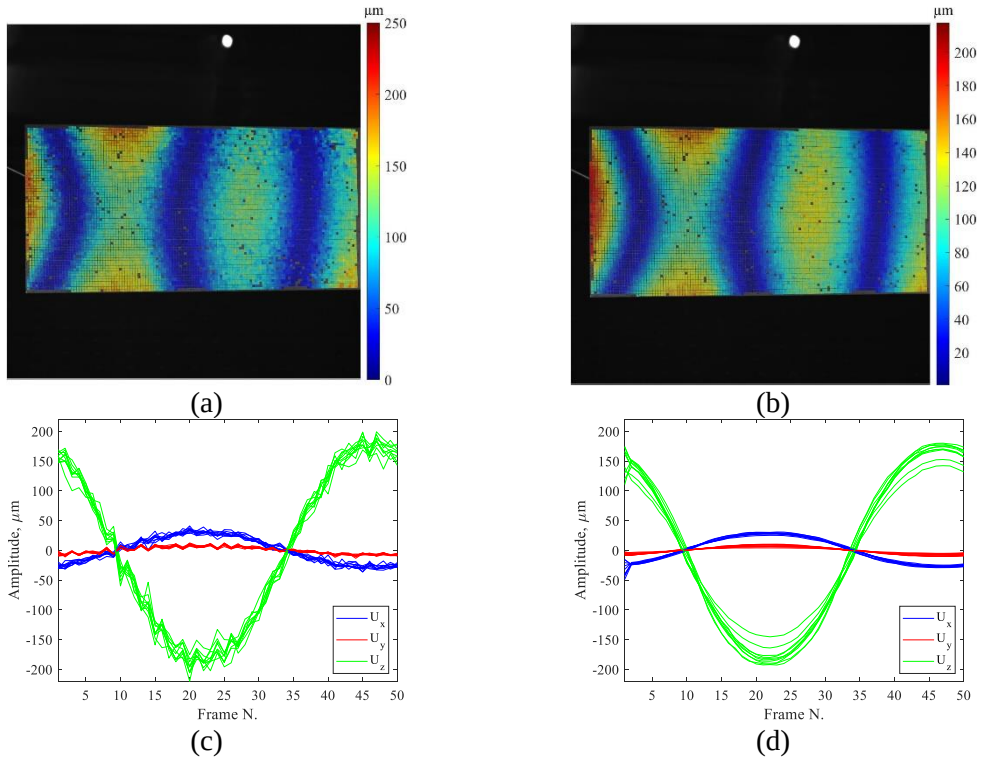

Figure 6. Map of the high amplitude displacement: (a) unfiltered image set, (b) filtered image set. Three displacement components overtime of the plate's free end: (c) unfiltered image set and (d) filtered image set.

This first example already allows assessing the effect of the filter. Nevertheless, the test was repeated with ten times lower input voltage to the shaker, which results in small amplitude vibrations. Figure 7 shows the obtained results: Fig. 7(a) refers to the analysis of the unfiltered image set for 0.1 V excitation, showing a poor description of the displacement map. In addition, Fig. 7(c) shows the results for an even lower excitation of 0.05 V, which almost does not allow to define the deformed shape. On the other hand, Fig. 7(b) and Fig. 7(d) both refer to the elaboration of the filtered image sets for 0.1 V and 0.05 V, respectively. In both cases, it is still possible to assess the deformed shape of the

object, coherently with the deformation shown in Fig. 6, even if the maximum displacement amplitude is 25 μm (0.1 V excitation) and 12 μm (0.05 V excitation), thus fully validating the effectiveness of the proposed filter.

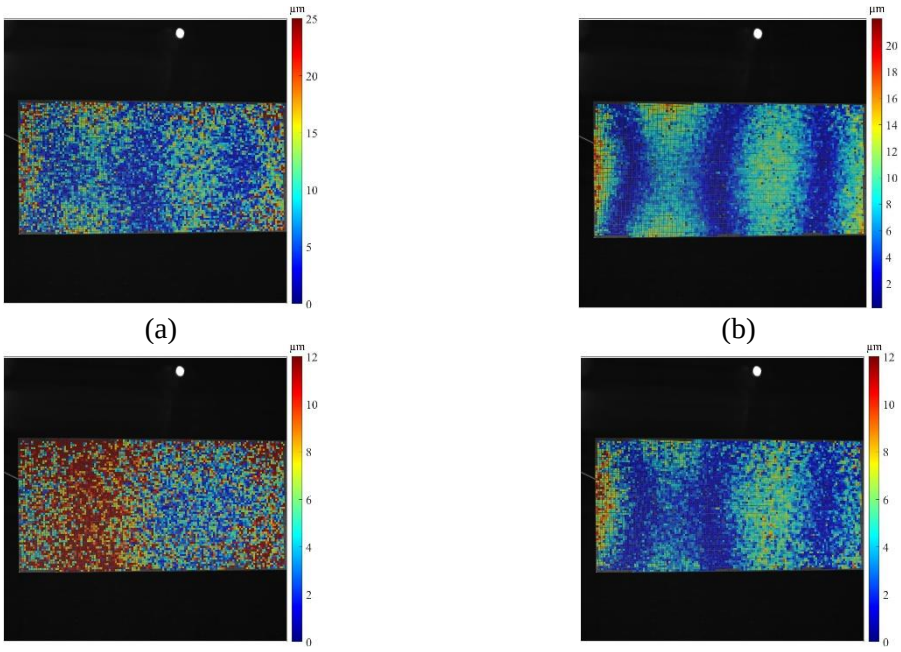

Figure 7. Elaboration at lower excitation amplitudes: (a) and (c) referring to the unfiltered image sets at 0.1 V and 0.05 V, respectively, and (b) and (d) referring to the filtered image sets 0.1 V and 0.05 V, respectively.

4.2. High-frequency application

Once the method was validated, it was tested on a realistic engineering application. A blisk with a maximum diameter of 200 mm and eleven blades was mounted on the shaker plate. Due to the peculiar shape of this component, the results were interpreted in a polar coordinate system centered on the blisk axis. A high-frequency excitation was imposed at 6458 Hz. Even if the shaker was set to the highest available load level, the maximum displacement amplitude was in the range of 10 μm, being high-frequency modes usually characterized by smaller amplitudes. This experimental configuration thus results in a challenging measurement task. The processing of the unfiltered data set led indeed to noisy maps, which did not allow to describe the deformed shape properly. On the other hand, Fig. 8 shows the results obtained by analyzing the filtered data set. More precisely, Fig. 8(a) reports the tangential component of the displacement by presenting the frame with the maximum amplitude. The figure highlights that one of the blades shows a dominant response, with respect to the others, which appear almost stationary according to this color scale. This is a common issue of blisks affected by mistuning due to machining tolerances, which shows asymmetric responses, especially at high frequencies. A deeper insight into the deformed shape can be obtained by further accentuating the color map to highlight the low amplitude displacements. This is done in Fig. 8(b), where the colormap was set in the range -5 / 5 μm. After this scale editing, it is possible to assess that the deformed shape is the same for all the blades, but with much smaller amplitudes with respect to the main one. Moreover, this measurement demonstrates that the described system, combined with the proposed time-domain filtering, can even measure displacements down to approximately 5 μm at frequencies higher than 6000 Hz.

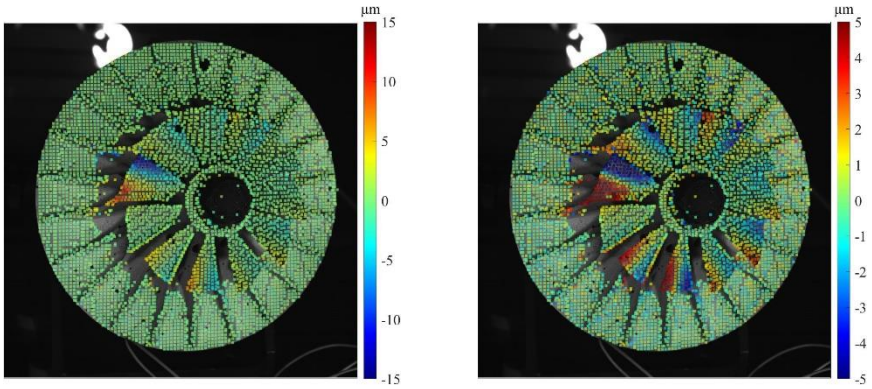

(a) (b)

Figure 8. Displacement amplitude map of the investigated blisk: (a) evidence of a single blade with larger displacement caused by mistuning, and (b) color map rescaled for highlighting the displacements of all the other blades.

5. Conclusion

This paper presents a filtering technique for pre-processing the left and right camera images then exploited for the 3D-DIC analysis. This filter can be combined with the down-sampling technique, which allows capturing high vibration frequencies even without high-speed cameras. Both the presented filter and the down-sampling approach require a purely sinusoidal signal. After acquiring a certain number of down-sampling (fictious) periods, the proposed filtering is based on the FFT decomposition and then the signal reconstruction with the Inverse FFT, but discarding all those harmonics that provide noise only. In other words, the harmonics to be preserved are the zero-order and the harmonic of the same order as the number of down-sampling periods, which usually is just one.

In the paper, the effectiveness of this filter is initially presented on a flexible cantilever plate setup, excited with a shaker at a relatively low frequency. The contents of each harmonic are presented in detail, and the filtering performance is evident by comparing the 3D-DIC with either the unfiltered and the filtered images. Within this application, the filter effectiveness was also tested by significantly reducing the shaker excitation intensity. A large noise overwhelming the signal was initially experienced, while the same vibration shape of the higher excitation was then observed after applying the filter. An accurate result was also obtained with a blisk excited at 6458 Hz for investigating the mistuning. The down-sampling was quite effective in this application, even at this high frequency, exploiting the minimum exposure time of 2 µs of the cameras. Small displacements were obviously obtained at this frequency, ranging from -15 to 15 µm and the vibrations of almost still blades were eventually highlighted by reducing the observation range from -5 to 5 µm. Even for these limited displacement levels, combined with very high frequency, clear displacement maps with accurate contours were again obtained.

References

[1] Sutton M A, Orteu J-J and Schreier H 2009 *Image Correlation for Shape, Motion and Deformation Measurements: Basic Concepts,Theory and Applications* (New York, N.Y.: Springer Publishing Company, Incorporated)

[2] Beberniss T J and Ehrhardt D A 2017 High-speed 3D digital image correlation vibration measurement: Recent advancements and noted limitations *Mech Syst Signal Pr* **86** 35-48

[3] Reu P L, Rohe D P and Jacobs L D 2017 Comparison of DIC and LDV for practical vibration and modal measurements *Mech Syst Signal Pr* **86** 2-16
[4] Yu L P and Pan B 2017 Full-frame, high-speed 3D shape and deformation measurements using stereo-digital image correlation and a single color high-speed camera *Opt Laser Eng* **95** 17-25
[5] Yu L P and Pan B 2017 Single-camera high-speed stereo-digital image correlation for full-field vibration measurement *Mech Syst Signal Pr* **94** 374-83
[6] Durand-Texte T, Simonetto E, Durand S, Melon M and Moulet M H 2019 Vibration measurement using a pseudo-stereo system, target tracking and vision methods *Mech Syst Signal Pr* **118** 30-40
[7] Barone S, Neri P, Paoli A and Razionale A V 2019 Low-frame-rate single camera system for 3D full-field high-frequency vibration measurements *Mech Syst Signal Pr* **123** 143-52
[8] Neri P, Paoli A and Santus C 2021 Stereo-DIC Measurements of a Vibrating Bladed Disk: In-Depth Analysis of Full-Field Deformed Shapes *Applied Sciences* **11**
[9] Warburton J R, Lu G, Buss T M, Docx H, Matveev M Y and Jones I A 2016 Digital Image Correlation Vibrometry with Low Speed Equipment *Exp Mech* **56** 1219-30
[10] Zhou Y H, Sun C, Song Y T and Chen J B 2015 Image pre-filtering for measurement error reduction in digital image correlation *Opt Laser Eng* **65** 46-56
[11] Pan B 2013 Bias error reduction of digital image correlation using Gaussian pre-filtering *Opt Laser Eng* **51** 1161-7
[12] Baldoni J, Lionello G, Zama F and Cristofolini L 2016 Comparison of different filtering strategies to reduce noise in strain measurement with digital image correlation *J Strain Anal Eng* **51** 416-30
[13] Mazzoleni P, Matta F, Zappa E, Sutton M A and Cigada A 2015 Gaussian pre-filtering for uncertainty minimization in digital image correlation using numerically-designed speckle patterns *Opt Laser Eng* **66** 19-33
[14] Becker T H and Marrow T J 2021 A Robust Finite Element-based Filter for Digital Image and Volume Correlation Displacement Data *Exp Mech*
[15] Wu R, Zhang D S, Yu Q F, Jiang Y X and Arola D 2019 Health monitoring of wind turbine blades in operation using three-dimensional digital image correlation *Mech Syst Signal Pr* **130** 470-83
[16] Barone S, Neri P, Paoli A and Razionale A V 2020 3D acquisition and stereo-camera calibration by active devices: A unique structured light encoding framework *Opt Laser Eng* **127**
[17] Eberl C 2010 Digital Image Correlation and Tracking. (Matlab Central: Mathworks)
[18] Neri P, Paoli A, Razionale A V and Santus C 2022 Low-speed cameras system for 3D-DIC vibration measurements in the kHz range *Mech Syst Signal Pr* **162** 108040